



# Subglacial lake activity beneath the ablation zone of the Greenland Ice Sheet

Yubin Fan<sup>1,2,3</sup>, Chang-Qing Ke<sup>1,2,3\*</sup>, Xiaoyi Shen<sup>1,2,3</sup>, Yao Xiao<sup>1,2,3</sup>, Stephen J. Livingstone<sup>4</sup>, Andrew J. Sole<sup>4</sup>

5 <sup>1</sup>Jiangsu Provincial Key Laboratory of Geographic Information Science and Technology, Key Laboratory for Land Satellite Remote Sensing Applications of Ministry of Natural Resources, School of Geography and Ocean Science, Nanjing University, Nanjing, 210023 China.

<sup>2</sup>Collaborative Innovation Center of Novel Software Technology and Industrialization, Nanjing, 210023 China.

<sup>3</sup>Collaborative Innovation Center of South China Sea Studies, Nanjing, 210023 China.

10 <sup>4</sup>Geography Department, University of Sheffield, Sheffield, UK, S10 2TN.

*Correspondence to:* Chang-Qing Ke (kecq@nju.edu.cn)

**Abstract.** Hydrologically active subglacial lakes can drain large volumes of water and sediment along subglacial pathways, affecting the motion and mass balance of ice masses, and impacting downstream sediment dynamics. Only seven active lakes have been reported beneath the Greenland Ice Sheet (GrIS) to date, and thus a systematic understanding of their spatial distribution and dynamic processes is still lacking. Here, using the ICESat-2 ATL11 data, we identified 61 active subglacial lakes, 15 59 of which have not been previously reported. The identification of active subglacial lakes beneath the GrIS is complicated by the occurrence of supraglacial lakes, which also fill and drain, and are hypothesized to be almost co-located. However, the ability of ICESat-2 to penetrate through shallow surface water allowed us to correct the elevation provided by the ATL11 data. A significant localized elevation anomaly was still measured in all detected subglacial lakes after correction, revealing that 18 subglacial lakes are twinned with supraglacial lakes. The active subglacial lakes have large upstream hydrological catchments and are located near or below the equilibrium line. These observations suggest that active subglacial lakes are widespread components of the subglacial drainage system and provide critical information for understanding their activity.

## 1 Introduction

Subglacial lakes that fill and drain on annual to decadal timescales are termed hydrologically active subglacial lakes (henceforth ‘active’). These lakes transiently store and then release water downstream, lubricating the ice-bed interface and affecting ice sheet mass balance by changing the ice discharge speed (Siegfried & Fricker, 2018; Malczyk et al., 2020). Some active subglacial lakes are hydraulically connected to other lakes, and water exchange between lakes can impact hydraulic gradients and subglacial water flow (Smith et al., 2017). Lake drainage not only exchanges water between lakes, but also transfers sediment and nutrients downstream, feeding microbial communities (Vick-Majors et al., 2020). Water crossing the 30 grounding line can also reduce the stability of ice shelves (Li et al., 2021). Therefore, knowledge of the distribution and water budget of active subglacial lakes is vital for understanding the stability of ice sheets.



Subglacial lakes can be identified from various remote sensing observations. Seismic and gravity inversions of lakes can determine their bathymetries and characterize their geological properties (Studinger et al., 2004). Additionally, subglacial lakes produce a flat ice-bed interface with high reflectance in radargrams and can therefore be recognized from radar echo sounding (RES) (Wright et al., 2012; Palmer et al., 2013; Bowling et al., 2019; Bessette et al., 2021; Maguire et al., 2021). Water that moves in and out of subglacial lakes can lead to localized ice-sheet surface deformation, enabling their corresponding volume changes to be studied through localized height anomalies detected from satellite radar (Siegfried & Fricker, 2018), laser altimeters (Smith et al., 2009; Siegfried & Fricker, 2021), and multi-temporal optical (Palmer et al., 2015) and radar interferometry-based Digital Elevation Models (DEMs) (Gray et al., 2005).

More than 675 subglacial lakes have been detected underneath the Antarctic Ice Sheet (Livingstone et al., 2022), including more than 130 active lakes (Smith et al., 2009; 2017). Conversely, only 7 active and 57 stable subglacial lakes have been identified underneath the Greenland Ice Sheet (GrIS) (Livingstone et al., 2022), although hydrologic potential calculations indicate that subglacial lakes could account for approximately 1.2% of the GrIS area (Livingstone et al., 2013). Constrained by steeper ice surface slopes and thus stronger hydraulic gradients, lakes underneath the GrIS tend to be smaller (Bowling et al., 2019), making it difficult for satellite altimeters (e.g., ICESat and CryoSat-2) to study subglacial lake activity in detail due to their coarse spatial or temporal resolutions. The few active lakes underneath the GrIS were identified from multi-temporal DEMs (Palmer et al., 2015; Howat et al., 2015; Bowling et al., 2019; Livingstone et al., 2019).

ICESat-2 has an improved footprint size (approximately 17 m with 0.7 m along-track) and spatial coverage ( $\pm 88^\circ$  latitudes) compared to previous satellite altimeters, providing an essential dataset for enabling active subglacial lake detection across the GrIS. Furthermore, its 91-day revisit cycle has the ability to reveal how the basal water system operates on sub-annual timescales. This study aims to detect active GrIS subglacial lakes by measuring ice-surface elevation anomalies observed from ICESat-2 between March 2019 and December 2020. Subglacial lakes were confirmed and their boundaries identified using the ArcticDEM (Porter et al. 2018). Spatial patterns of elevation and volume changes over the combined ArcticDEM and ICESat-2 periods (2009-2020) were used to determine the temporal patterns of lake activity.

## 2 Data

### 2.1 ICESat-2 data

Time series of ice surface heights derived from the ICESat-2 ATL11 (Version 3) product (Smith et al., 2021) were used to study active subglacial lakes. The product contains ice surface elevations for repeat observations along each ICESat-2 reference ground track (RGT) from cycle to cycle (91 days apart) in polar regions (poleward of  $60^\circ$  N and  $60^\circ$  S), accompanied by geolocation information and the corresponding quality assessment. The three beam pairs of ICESat-2 follow a reference pair track (RPT) parallel to the RGT, with the reference points of the ATL11 product spaced along each RPT. The ATL11 product is posted at a spatial resolution of 60 m, with the spacing of tracks within each RGT ranging from approximately 5.4 km (high



latitude) to 7.4 km (low latitude). More information on the ATL11 data and its processing algorithm can be found in Smith et al. (2021).

65 The ICESat-2 ATL11 v3 product contains ice surface elevations with respect to the WGS84 ellipsoid from March 2019 to December 2020 (i.e., cycles 3-9) for each reference point. In total, the elevation measurements of all 511 RGTs (1533 RPTs, 2638 track segments) were used to detect active subglacial lakes and explore their elevation and volume changes from 2019 to 2020. We collected  $2.91 \times 10^7$  reference points over the entire of Greenland. Only data with cycles marked as good quality (quality\_summary=0) were used, leading to an overall spatial density of  $1.34 \times 10^5$  points per square kilometer. Finally, ATL03  
70 data, which contain the full stream of returned photons (Neumann et al., 2019), were used to identify surface meltwater and correct the ice surface elevation measurements for its presence during the melt season.

## 2.2 Validation data

The ArcticDEM is a high-resolution, high-quality digital surface model (DSM) of the Arctic based on optical stereo imagery from GeoEye-1 and WorldView-1/2/3 (Porter et al., 2018), and with an internal accuracy of 0.2 m (Noh & Howat, 2015). The  
75 2-m resolution strip DSM files provided elevation measurements from August 2009 to March 2017. The temporal resolution of these time-stamped DSM segments was variable due to the influence of clouds and shadows. However, the time-stamped strip ArcticDEM dataset allows the detection of localized elevation-change anomalies, and was used for lake cross-validation and boundary extraction. Published Greenland subglacial lake locations (Livingstone et al., 2022) were also used for validation.

## 3 Methods

### 80 3.1 Identification of active subglacial lakes

Subglacial lakes were detected from localized ice-surface height anomalies measured by ICESat-2. The elevation-change rate of individual reference points was obtained through a linear fit by using the timestamp and elevation value of valid elevation measurements (e.g., Figure 1a). We then generated a Greenland-wide elevation change trend map by gridding these point trend data at a resolution of 500 m, which covers approximately 80% of the GrIS. We did not interpolate the cells to reduce the  
85 potential misidentification of subglacial lakes. The change map was used to create masks for candidate regions. Previous studies used a threshold of  $\pm 0.5$  m/yr to select regions with a significant localized elevation change in Antarctica (Fricker et al., 2007; Smith et al., 2017; Malczyk et al., 2020), but knowledge of such a threshold applicable to Greenland subglacial lakes is lacking. We adopted a more conservative threshold  $\pm 0.2$  m/yr to identify potential subglacial lakes that could then be verified using the ArcticDEM dataset and through manual examination of ice-surface elevation patterns.

90 The elevation-change anomaly associated with subglacial lake filling and/ or drainage should have a characteristic spatial pattern comprising an obvious elevation anomaly at the lake center while the outside remains stable. Candidate regions where the elevation anomaly can be explained by other factors, including displacement of the footprints, dynamic topography, and



cloud cover, etc., were discarded (Smith et al., 2009). The elevation profiles were used to determine lake location by visual interpretation (Willis et al., 2015) (e.g., Figures 1b, c).

### 95 3.2 ArcticDEM validation and lake boundary determination

Time-series of time-stamped ArcticDEM data were used to cross-validate subglacial lake locations. Areas of known subglacial lakes in Greenland range from 0.18 to 8.4 km<sup>2</sup>, with a maximum length of 1.6 km (Livingstone et al., 2022). Therefore, a 5 km radius circular buffer was established around the point at the center of the potential lake determined from the ICESat-2 data, which was taken as the maximum possible extent of the subglacial lake. To provide spatially continuous images and  
100 improve computational efficiency, we derived the median value of the DSMs every 100 days to obtain the elevation maps. Then, we calculated the elevation difference between each temporally adjacent elevation map, which was used to determine whether there was an elevation anomaly (e.g., Figure 1a). Subglacial lakes which also coincided with elevation anomalies during the ArcticDEM period were confirmed as subglacial lakes. We acknowledge that the time differences between ICESat-2 and ArcticDEM data might affect the percentage of confirmed lakes because some lakes did not show full drainage or filling  
105 activity.

The large spacing of tracks (5-7 km, exceeding the lake size) make it difficult to extract the subglacial lake boundary by generating an elevation-change surface through interpolation of the ICESat-2 data. Therefore, the boundary was manually delineated from the ArcticDEM elevation-change anomaly maps. We still retained subglacial lakes that were not identified from the ArcticDEM, to analyze the spatial pattern and elevation-change rate, but eliminated them from our analysis of volume  
110 change and long-term lake activity.

### 3.3 Impact of surface lakes on the detection of subglacial lakes

In much of the ablation zone of the GrIS numerous supraglacial lakes seasonally form and then either freeze or drain over the ice surface or to the bed (Selmes et al., 2011). The filling and drainage of these lakes produces ice-surface elevation anomalies in the ATL06 product (and therefore the ATL11 product) that could be mis-classified as subglacial lake activity. This is  
115 particularly challenging because supraglacial and subglacial lakes are hypothesized to exist in tandem (Sergienko, 2013).

To discriminate between surface and subglacial lakes we first evaluated the temporal pattern and magnitude of the ice-surface elevation changes. Supraglacial lakes often drain rapidly to the bed in the summer via moulins (MacFerrin et al., 2019), and are therefore characterized by a seasonal fill-drain pattern, whereas subglacial lakes tend to fill over multiple years. Supraglacial lakes are also typically shallow features (Pope et al., 2016) and so large elevation anomalies (>10 m) are more  
120 likely to be caused by subglacial lake drainages. A key advantage of ICESat-2 is that the ATL03 photon data can penetrate surface meltwater as deep as 7 m (Fair et al., 2020) producing a double reflection of both the water surface and ice surface beneath (Fricker et al., 2020). For each potential subglacial lake, we were therefore able to identify whether there was a double reflection and apply the Watta algorithm to discriminate the supraglacial lake surface and bottom (Datta et al., 2021). The



125 bottom height was taken as the corrected ATL11 elevation and used to recalculate the elevation change rate for subglacial lake footprints within each supraglacial lake (Figure S1). This correction was applied to 18 subglacial lakes, and in all cases a significant localized elevation anomaly was still measured indicating that ~30% of active subglacial lakes in this study are twinned with surface lakes.

### 3.4 Lake confidence level classification

130 We classified these potential lakes into three confidence levels. Low confidence lakes exhibited no clear pattern of multi-year elevation change with time, might be associated with flat surfaces and annual elevation cycles that could be the expression of surface lakes, had a limited number of data points, and a small maximum signal change (<10 m change). High confidence lakes were identified from >10 m ice-surface elevation change, a clear double reflector or no evidence of surface water, and an elevation change pattern typical of subglacial lakes (e.g., multi-year pattern of filling and then rapid drainage). Medium confidence lakes had an elevation change pattern typical of subglacial lakes, but a less clear signal, for example a smaller ice-surface elevation change, fewer data points or some flat surfaces. We discounted the low confidence potential lakes as likely  
135 to be caused by other processes (e.g., filling and draining of surface lakes).

### 3.5 Estimation of lake elevation and volume change

The median elevation-change rate during the ICESat-2 period was first calculated for all the lake polygons. As this rate is composed of ice-flux divergence, ice ablation and water motion (Smith et al., 2009), the median elevation-change rate of the  
140 area surrounding the lake (within a buffer-region) was subtracted to isolate the relative elevation-change effect of the subglacial lake. Here, we defined a circular buffer region outside each lake boundary with a width equal to the radius of a circle whose area is equal to the lake. To quantify the effect of buffer-region width on the elevation-change rate, we tested two other width buffers: (1) a fixed buffer of 2 km; and (2) a buffer of half the radius of the standard buffer (Table S1). The mean value of the absolute differences between the two adapted buffers was approximately 0.16 m, which only accounts for 6.5% of the averaged  
145 absolute elevation-change rate. Therefore, the effect of the buffer size on the elevation-change rate was neglected. For the unconfirmed lakes, we used half of the along-track distance where the elevation anomaly was detected as a buffer.

A boundary that encompassed all elevation-change anomalies was then defined, and we defined the corrected elevation change rate,  $dh_c$  for each lake as shown in Equation 1:

$$dh_c = dh_{median,inside} - dh_{median,outside} \quad (1)$$

150 where  $dh_{median,inside}$  is the median elevation-change rate of ATL11 footprints within each lake's bounding polygon, and the  $dh_{median,outside}$  is defined as the median value of the elevation change rate for ATL11 footprints outside the bounding polygon but within the buffer zone.



The uncertainty of the elevation-change rate was calculated by the standard deviations of the elevation-change rates of all footprints inside and outside the lake polygon, defined in Equation 2.

$$155 \quad dh_{c,uncertainty} = \sqrt{dh_{std,inside}^2 + dh_{std,outside}^2} \quad (2)$$

The volume change rate was derived by integrating the elevation change rate and lake boundary for the confirmed lakes (Equation 3). To estimate the errors in our volume change estimates caused by boundary migration, we assumed an area uncertainty of one grid cell of the ArcticDEM differencing image (i.e., 30 m x 30 m) and calculated the volume change uncertainty as shown in Equation 4.

$$160 \quad dV_{confirmed} = dh_c \times area \quad (3)$$
$$dV_{confirmed,uncertainty} = \sqrt{(dh_{c,uncertainty} \times area)^2 + (dh_c \times area_{uncertainty})^2} \quad (4)$$

For the unconfirmed lakes we only calculated elevation change and its uncertainty because the boundaries could not be determined.

### 3.6 Lake activity recognition

165 To remove the influence of systematic vertical and horizontal offsets between ArcticDEMs, we calculated the relative height anomaly by subtracting the averaged ice-surface elevation within the lake from the buffer around it (Livingstone et al., 2019). We used the same method to calculate the relative height anomaly, and then combined the ArcticDEM and ICESat-2 periods (2009-2020) to determine the temporal patterns of lake activity. Each of the DSMs was corrected against filtered ICESat altimetry data using the metadata provided. As we calculated the relative height anomaly we used the internal accuracy of the  
170 data as a measure of uncertainty. The internal accuracy of the ArcticDEM is 0.2 m (Noh & Howat, 2015), and 0.09 m for ICESat-2 footprints (Brunt et al., 2019).

## 4. Results

### 4.1 Cross-validation of subglacial lake location

Using ICESat-2, we identified 15 high confidence and 46 medium confidence active lakes (61 in total). A total of 51 identified  
175 active lakes were confirmed by the ArcticDEM data (Figure 2a). Two previously identified active subglacial lakes were also identified in this study, located at the Flade Isbink Ice Cap (Willis et al., 2015) and Inuppaat quaat (Howat et al., 2015; Palmer et al., 2015). An additional 10 active lakes were detected by ICESat-2 but not the ArcticDEM timeseries, and 5 reported active lakes were missed by ICESat-2, indicating that these lakes may be transient features or in a relatively steady state during the corresponding periods. No classic bright, flat and strong reflections were found from analysis of RES data for the 61 active



180 lakes identified in this study. This mismatch between RES- and altimeter-detected lakes has also been reported in Antarctica (Siegert et al., 2014).

#### 4.2 Distribution of active subglacial lakes

Of the 61 active subglacial lakes identified over the entire GrIS, 27 lakes were covered several times, but by only one RPT. The well-sampled subglacial lakes covered by 3-4 RPTs are located in northernmost Greenland. However, since lakes occur  
185 at all latitudes, we infer that their occurrence has no connection with the spatial density of ICESat-2 tracks. We adopted informal names for these lakes (Table S2) based on the Greenland basin name (Mouginot et al., 2019).

Active subglacial lakes are concentrated toward the ice margin and have large upstream subglacial hydrologic catchments (Figure 2a). Three main clusters of active lakes were observed in northwestern, northern, and southwestern Greenland, corresponding to regions of significant negative surface mass balance (Khan et al., 2022) and where surface meltwater can  
190 access the bed due to limited firn and the occurrence of moulins and crevasses. This distribution is consistent with that predicted in Bowling et al. (2019), with hydrologically active lakes located near or below the Equilibrium Line Altitude (ELA). There is a general paucity of active lakes in the southeastern sector of Greenland where high accumulation rates and thick firn limit the amount of surface-derived water that reaches the ice bed, and inland sectors of Greenland, where the bed is thought to be largely frozen (MacGregor et al., 2022). In contrast, stable subglacial lakes tend to be located in northern and eastern regions  
195 above the ELA (Bowling et al., 2019). Active lakes are typically located near regions of fast ice flow (>50 m/yr) (Figure S2) and 51 of them are within marine-terminating catchments. This distribution is consistent with the spatial pattern found in Antarctica (Smith et al., 2009).

The active subglacial lakes identified in this study differ in size from those observed in Antarctica, reflecting the different topographic setting, and steeper ice-surface slopes and thus hydrologic gradients controlling the morphology of subglacial  
200 lakes (see also Bowling et al., 2019). Lake area ranges from 0.20 to 16.23 km<sup>2</sup>, with an average area of 3.11 km<sup>2</sup> (Figure 2b). Approximately 25% of the subglacial lakes have an area < 1 km<sup>2</sup>, indicating that small lakes are prevalent throughout Greenland. Only one lake situated in Basin USULLUUP SERMIA was > 10 km<sup>2</sup> (see Figure S3). The areas of unconfirmed lakes were comparable to those of confirmed lakes based on analysis of their diameter along the ICESat-2 tracks.

#### 4.3 Elevation change and water budget

205 The elevation range can provide important information on lake depth. By combining the elevation time-series of the ArcticDEM and ICESat-2 data to give a maximum lake depth estimation for the 51 confirmed lakes, we show that 9 lakes have a lake depth of less than 10 m, 27 lakes have a depth between 10 and 30 m, and only 3 lakes have greater than 50 m depth (Figure S4).

Generally, active subglacial lakes in Greenland exhibit higher elevation change rates (usually larger than 1 m/yr) than those in  
210 Antarctica. Positive temporal elevation trends were identified in 59% of the lakes detected during 2019-2020 (Figure 2c),





indicating net water recharge. Lakes with both positive and negative elevation change rates during the study period were found in each basin with few exceptions. The absolute elevation-change rates ranged from 0.01 to 16.03 m/yr with a mean value of 3.26 m/yr. The largest elevation changes tended to occur in the lake center, reducing outwards to the boundary. The uncertainty of the elevation-change rate generally depended on the number of footprints, the slope of the lake bed, and the acquisition time  
215 of different tracks, and ranged from 0.32 to 8.09 m/yr with a mean value of 2.76 m/yr.

Our ability to estimate volume change depended on the location and size of the lake in relation to the ICESat-2 tracks that detected the elevation anomalies. Large lakes tended to have faster volume-change rates than small lakes (with a correlation coefficient of 0.44,  $p < 0.001$ ), suggesting that they have a greater impact on the subglacial hydrological system (Livingstone et al., 2022). Lake volume change exhibited the same spatial pattern as the elevation change, with most lakes displaying a  
220 positive volume change over the observation period of ICESat-2 (Figure 2d). The absolute volume change rates ranged from  $1.1 \times 10^4$  to  $5.17 \times 10^7$  m<sup>3</sup>/yr with a mean value of  $7.74 \times 10^6$  km<sup>3</sup>/yr (Table S2). Volume change rate uncertainties ranged from  $4 \times 10^4$  to  $1.31 \times 10^7$  km<sup>3</sup>/yr, with a mean value of  $3.82 \times 10^6$  km<sup>3</sup>/yr.

## 5. Discussion

### 5.1 Dynamic processes of active subglacial lakes

225 Variable subglacial lake activity was detected by ICESat-2 during 2019-2020 (Figure 3). Thirty-five lakes exhibited only filling or draining throughout the study period. In contrast, only 6 lakes experienced at least 3 abnormal elevation changes during 2019-2020 (Table S2). A total net positive volume change rate of 0.10 km<sup>3</sup>/yr was found for the detected active subglacial lakes. Recharge of these subglacial lakes is thought to be generated from geothermal heat flux, frictional heating from ice flow and surface meltwater inputs (Bowling et al., 2019). As all 61 active lakes are located near or below the  
230 equilibrium line in areas of high negative surface mass balance, we hypothesise that surface meltwater runoff which reaches the ice bed has a strong control on lake activity (see also Liang et al., 2022). However, the relationship between positive volume change rate and runoff estimates from the high-resolution Regional Atmospheric Climate Model (RACMO2.3p2) (Noël et al., 2018) revealed only a slight positive correlation (with a correlation coefficient of 0.38,  $p < 0.1$ ). This unclear relationship might reflect the relatively coarse temporal resolution of our data during individual melt seasons (cf. Liang et al., 2022), but  
235 still provides a hint that active lakes in Greenland are predominantly recharged by surface melt.

### 5.2 Lake activity: fill-drain patterns

Livingstone et al. (2022) classified subglacial lake activity into 5 temporal patterns based on the ratio of filling and draining durations. They found that 3 active subglacial lakes in Greenland exhibited quiescence at high stand. To further improve the understanding of dynamic hydrological processes underneath the GrIS, we used the combination of ArcticDEM and ICESat-  
240 2 to measure the fill–drain patterns of active lakes over 11 years.





The temporal resolution of the ArcticDEM varies making it difficult to discriminate clear fill-drain patterns for all lakes. However, in total we identified 20 lakes with specific fill–drain cycles (Table S2). One lake exhibited slow filling and rapid draining (Figure 3a), one lake exhibited similar rates of filling and draining (Figure 3b), with 15 lakes quiescent at high stand (Figure 3c) and 3 lakes quiescent at low stand (Figure 3d). The dominance of lakes quiescent at high stand provides further support for an external threshold controlling the initiation of lake drainage in Greenland (Livingstone et al., 2022). Twenty-nine of 41 drainage events happened between May and August (Table S3), with 2 lakes draining between December and February (e.g., KONG\_OSCAR\_GLETSCHER02). The tendency for lakes to drain in summer also supports the idea that surface meltwater can influence or trigger drainage.

## 6. Conclusions

We used ICESat-2 altimetry to detect active subglacial lakes underneath the Greenland Ice Sheet and to discriminate their signal from surface lake drainage patterns. Multi-temporal ArcticDEM strip maps were used to extend the timeseries, allowing us to help verify lakes and their drainage history. In total, we identified 59 new active lakes, more than 8 times the previous number. Lakes are concentrated toward the ice margin, and correspond with regions of significant negative surface mass balance. This distribution indicates that the formation and dynamism of active lakes in Greenland is related to the ability of surface-derived meltwater to access the ice bed (i.e., little snow/firn and lots of crevasses and/or moulins). Thirteen of the subglacial lakes had an area  $< 1 \text{ km}^2$ , and only one lake had an area  $> 10 \text{ km}^2$ , but large lakes exhibited faster volume-change rates than small lakes, suggesting that they have a greater impact on the subglacial hydrological system. Finally, lake drainages typically occur in the summer melt season, and 15 of the 20 lakes where clear fill-drain cycles were identified displayed long-term quiescence at high stand followed by drainage, suggesting surface melt might control the initiation of subglacial lake drainage in Greenland.

## Author contributions

Yubin Fan performed the identification of active lakes and wrote the manuscript; Chang-Qing Ke contributed to the conception of the study and supervised the work; Xiaoyi Shen contributed to the discussion and advised on the elevation change and water budget; Yao Xiao performed ArcticDEM validation on Google Earth Engine (GEE) platform. Stephen J. Livingstone and Andrew J. Sole revised the manuscript and advised on lake confidence level classification. All authors contributed to the discussion of the results and to the improvement of the manuscript.

## Competing interests

The authors declare that they have no conflict of interest.



## Acknowledgements

270 This work was supported by the Program for National Natural Science Foundation of China (grant No. 41830105 & 42011530120). ICESat-2 data (<https://nsidc.org/data/ATL11/versions/3>) were obtained from the National Snow and Ice Data Center. The ArcticDEMs were obtained and processed in the GEE platform (<https://code.earthengine.google.com/>). RACMO2.3p2 Greenland daily runoff data were kindly provided by Brice Noël and MAR data were kindly provided by Xavier Fettweis.

## 275 References

- Bessette, J. T., Schroeder, D. M., Jordan, T. M., and MacGregor, J. A.: Radar-sounding characterization of the subglacial groundwater table beneath Hiawatha Glacier, Greenland. *Geophys. Res. Lett.*, 48, e2020GL091432, <https://doi.org/10.1029/2020GL091432>, 2021.
- Bowling, J.S., Livingstone, S. J., Sole, A. J. and Chu, W.: Distribution and dynamics of Greenland subglacial lakes. *Nature Communications*, 10:2810, <https://doi.org/10.1038/s41467-019-10821-w>, 2019.
- 280 Brunt, K. M., Neumann T. A., and Smith B. E.: Assessment of ICESat-2 Ice Sheet Surface Heights, Based on Comparisons Over the Interior of the Antarctic Ice Sheet. *Geophys. Res. Lett.*, 46, 13,072–13,078, <https://doi.org/10.1029/2019GL084886>, 2019.
- Datta, R. T., and Wouters, B.: Supraglacial lake bathymetry automatically derived from ICESat-2 constraining lake depth estimates from multi-source satellite imagery. *The Cryosphere*, 15, 5115–5132, <https://doi.org/10.5194/tc-15-5115-2021>, 2021.
- 285 Fair, Z., Flanner, M., Brunt, K. M., Fricker, H. A., and Gardner, A.: Using ICESat-2 and Operation IceBridge altimetry for supraglacial lake depth retrievals. *The Cryosphere*, 14, 4253–4263, <https://doi.org/10.5194/tc-14-4253-2020>, 2020.
- Fettweis, X., Hofer, S., Séférian, R., Amory, C., Delhasse, A., Doutreloup, S., Kittel, C., Lang, C., Bever, J., Veillon, F., and Irvine, P.: Brief communication: Reduction of the future Greenland ice sheet surface melt with the help of solar geoengineering. *The Cryosphere*, 15, 3013–3019, <https://doi.org/10.5194/tc-15-3013-2021>, 2021.
- 290 Fricker, H. A., Scambos, T., Bindschadler, R., and Padman, L.: An active subglacial water system in West Antarctica mapped from space. *Science*, 315(5818), 1544–1548, <https://doi.org/10.1126/science.1136897>, 2007.
- Fricker, H. A., Arndt, P., Brunt, K. M., Datta, R. T., Fair, Z. and Jasinski, M. F.: ICESat-2 Meltwater Depth Estimates: Application to Surface Melt on Amery Ice Shelf, East Antarctica. *Geophys. Res. Lett.*, 48, e2020GL090550, <https://doi.org/10.1029/2020GL090550>, 2020.
- 295 Gray, L., Joughin, I., Tulaczyk, S. and Spikes, V. B.: Evidence for subglacial water transport in the West Antarctic Ice Sheet through three-dimensional satellite radar interferometry. *Geophys. Res. Lett.*, 32, L03501, <https://doi.org/10.1029/2004GL021387>, 2005.
- Howat, I. M., Porter, C., Noh, M. J., Smith, B. E. and Jeong, S.: Brief communication: sudden drainage of a subglacial lake beneath the Greenland Ice Sheet. *The Cryosphere*, 9, 103–108, <https://doi.org/10.5194/tc-9-103-2015>, 2015.
- 300



- Khan, S.A., Bamber, J.L., Rignot, E., Helm, V., Aschwanden, A., Holland, D.M., Broeke, M., King, M., Noël, B., Truffer, M., Humbert, A., Colgan, W., Vijay, S., and Munneke, P.: Greenland mass trends from airborne and satellite altimetry during 2011–2020. *J. Geophys. Res.: Earth Surf.*, 127(4), p.e2021JF006505, <https://doi.org/10.1029/2021JF006505>, 2022.
- Li, Y., Shi, H., Lu, Y., Zhang, Z. and Xi, H.: Subglacial discharge weakens the stability of the Ross Ice Shelf around the grounding line. *Polar Res.*, 40, 3377, <https://doi.org/10.33265/polar.v40.3377>, 2021.
- 305 Liang, Q., Xiao, W., Howat, I., Cheng, X., Hui, F., Chen, Z., Jiang, M., and Zheng, L.: Filling and drainage of a subglacial lake beneath the Flade Isblink ice cap, northeast Greenland. *The Cryosphere Discussions*, pp.1-17, <https://doi.org/10.5194/tc-2021-374>, 2022.
- Livingstone, S. J., Clark, C. D., Woodward, J. and Kingslake, J.: Potential subglacial lake locations and meltwater drainage pathways beneath the Antarctic and Greenland ice sheets. *The Cryosphere*, 7, 1721–1740, <https://doi.org/10.5194/tc-7-1721-2013>, 2013.
- 310 Livingstone, S. J., Sole, A. J., Storrar, R. D., Harrison, D., Ross, N., and Bowling, J.: Brief communication: Subglacial lake drainage beneath Isunguata Sermia, West Greenland: geomorphic and ice dynamic effects. *The Cryosphere*, 13, 2789–2796, <https://doi.org/10.5194/tc-13-2789-2019>, 2019.
- 315 Livingstone, S. J., Li, Y., Rutishauser, A., Sanderson, R. J., Winter, K., Mikucki, J. A., Björnsson, H., Bowling, J., Chu, W., Dow, C., Fricker, H., McMillan, M., Ng, F., Ross, N., Siegert, M., Siegfried, M., and Sole, A.: Subglacial lakes and their changing role in a warming climate. *Nat. Rev. Earth Environ.*, 19, <https://doi.org/10.1038/s43017-021-00246-9>, 2022.
- MacFerrin, M., Machguth, H., van As, D., Charalampidis, C., Stevens, C. M., Heilig, A., Vandecrux, B., Langen, P. L., Mottaram, R., Fettweis, X., Broeke, M., Pfeffer, W. T., Moussavi, M. S., and Abdalati, W.: Rapid expansion of Greenland’s low-permeability ice slabs. *Nature*, 573, 403–407, <https://doi.org/10.1038/s41586-019-1550-3>, 2019.
- 320 MacGregor, J. A., Chu, W., Colgan, W. T., Fahnestock, M. A., Felikson, D., Karlsson, N. B., Nowicki, S., and Studinger, M.: GBaTSv2: A revised synthesis of the likely basal thermal state of the Greenland Ice Sheet. *The Cryosphere Discussions*, pp. 1-25. <https://doi.org/10.5194/tc-2022-40>, 2022.
- Maguire, R., Schmerr, N., Pettit, E., Riverman, K., Gardner, C., DellaGiustina, D. N., Avenson, B., Wagner, N., Marusiak, A. G., Habib, N., Broadbeck, J. I., Bray, V. J., and Bailey, S. H.: Geophysical constraints on the properties of a subglacial lake in northwest Greenland, *The Cryosphere*, 15, 3279–3291, <https://doi.org/10.5194/tc-15-3279-2021>, 2021.
- 325 Malczyk, G., Gourmelen, N., Goldberg, D., Wuite, J., and Nagler, T.: Repeat subglacial lake drainage and filling beneath Thwaites Glacier. *Geophys. Res. Lett.*, 47, e2020GL089658, <https://doi.org/10.1029/2020GL089658>, 2020.
- Mouginot, J. and Rignot, E.: Glacier catchments/basins for the Greenland Ice Sheet.” UC Irvine Dash. <https://doi.org/10.7280/D1WT11>, 2019.
- 330 Noël, B., van de Berg, W. J., van Wessem, J. M., van Meijgaard, E., van As, D., Lenaerts, J. T. M., Lhermitte, S., Ligtenberg, S. R. M., Medley, B., Reijmer, C. H., Tricht, K., Trusel, L. D., van Ulf, L. H., Wouters, B., Wuite, J., and van den Broeke, M.R.: Modelling the climate and surface mass balance of polar ice sheets using RACMO2 – Part 1: Greenland (1958–2016), *The Cryosphere*, 12, 811-831, <https://doi.org/10.5194/tc-12-811-2018>, 2018.



- 335 Noh, M.J. and Howat, I. M.: Automated stereo-photogrammetric DEM generation at high latitudes: Surface extraction with TIN-based search-space minimization (SETSM) validation and demonstration over glaciated regions. *GISci Remote Sens*, 52, 198–217, <https://doi.org/10.1080/15481603.2015.1008621>, 2015.
- Palmer, S. J., Dowdeswell, J. A., Christoffersen, P., Young, D. A., Blankenship, D. D., Greenbaum, J. S., Benham, T., Bamber, J., and Siegert, M. J.: Greenland subglacial lakes detected by radar, *Geophys. Res. Lett.*, 40, <https://doi.org/10.1002/2013GL058383>, 2013.
- 340 Palmer, S., Mcmillan, M. and Morlighem, M.: Subglacial lake drainage detected beneath the Greenland ice sheet. *Nature Communications*, 6, 8408, <https://doi.org/10.1038/ncomms9408>, 2015.
- Pope, A., Scambos, T.A., Moussavi, M., Tedesco, M., Willis, M., Shean, D. and Grigsby, S.: Estimating supraglacial lake depth in West Greenland using Landsat 8 and comparison with other multispectral methods. *The Cryosphere*, 10(1), pp.15-27, <https://doi.org/10.5194/tc-10-15-2016>, 2016.
- 345 Porter, C., Morin, P., Howat, I., Noh, M.J., Bates, B., Peterman, K., Keeseey, S., Schlenk, M., Gardiner, J., Tomko, K. and Willis, M.: ArcticDEM. *Harvard Dataverse*, 1, pp.2018-30, <https://doi.org/10.7910/DVN/OHHUKH>, 2018.
- Selmes, N., Murray, T., and James, T. D.: Fast draining lakes on the Greenland Ice Sheet. *Geophys. Res. Lett.*, 38(15). <https://doi.org/10.1029/2011gl047872>, 2011.
- 350 Sergienko, O. V.: Glaciological twins: basally controlled subglacial and supraglacial lakes. *J. Glaciol.*, 59, 213, <https://doi.org/10.3189/2013JoG12J040>, 2013.
- Siegert, M. J., Ross, N., Corr, H., Smith, B., Jordan, T., Bingham, R. G., Ferraccioli, F., Rippin, M., and Le Brocq, A.: Boundary conditions of an active West Antarctic subglacial lake: implications for storage of water beneath the ice sheet. *The Cryosphere*, 8, 15–24, <https://doi.org/10.5194/tc-8-15-2014>, 2014.
- 355 Siegfried, M. R., and Fricker, H. A.: Thirteen years of subglacial lake activity in Antarctica from multi-mission satellite altimetry. *Ann. Glaciol.*, 59(76pt1), 42-55. <https://doi.org/10.1017/aog.2017.36>, 2018.
- Siegfried, M. R., and Fricker, H. A.: Illuminating active subglacial lake processes with ICESat-2 laser altimetry. *Geophys. Res. Lett.*, 48, e2020GL091089, <https://doi.org/10.1029/2020GL091089>, 2021.
- Smith, B., Fricker, H., Joughin, I., and Tulaczyk, S.: An inventory of active subglacial lakes in Antarctica detected by ICESat (2003–2008). *J. Glaciol.*, 55(192), 573–595, <https://doi.org/10.3189/002214309789470879>, 2009.
- 360 Smith, B. E., Gourmelen, N., Huth, A., and Joughin, I.: Connected subglacial lake drainage beneath Thwaites Glacier, West Antarctica. *The Cryosphere*, 11(1), 451-467, <https://doi.org/10.5194/tc-11-451-2017>, 2017.
- Smith, B., Dickinson, S., Jelle, B. P., Neumann, T. A., Hancock, D., Lee, J., and Harbeck, K.: ATLAS/ICESat-2 L3B Annual Land Ice Height, Version 4. Boulder, Colorado USA. NASA National Snow and Ice Data Center Distributed Active Archive Center, <https://doi.org/10.5067/ATLAS/ATL11.004>, 2021.
- 365 Studinger, M., Bell, R. E. and Tikku, A. A.: Estimating the depth and shape of subglacial Lake Vostok’s water cavity from aerogravity data. *Geophys. Res. Lett.*, 31, L12401. <https://doi.org/10.1029/2004GL019801>, 2004.



370 Vick-Majors, T. J., Michaud, A. B., Skidmore, M. L., Turetta, C., Barbante, C., Christner, B. C., Dore, J. E., Christianson, K.,  
Mitchell, A. C., Achberger, A. M., Mikucki, J. A., and Pris, J. C.: Biogeochemical connectivity between freshwater ecosyste  
ms beneath the West Antarctic ice sheet and the sub-ice marine environment. *Global Biogeochem. Cycles*, 34, e2019GB0064  
46. <https://doi.org/10.1029/2019GB006446>, 2020.

Willis, M. J., Herried, B. G., Bevis, M. G., and Bell, R. E.: Recharge of a subglacial lake by surface meltwater in northeast G  
reenland. *Nature*, 518(7538), 223-U165, <https://doi.org/10.1038/nature14116>, 2015.

375 Wright, A. P., and Siegert, M.: A fourth inventory of Antarctic subglacial lakes, *Antarctic Science*, 24 (6), 659–664, <https://doi.org/10.1017/S095410201200048X>, 2012.



Figures

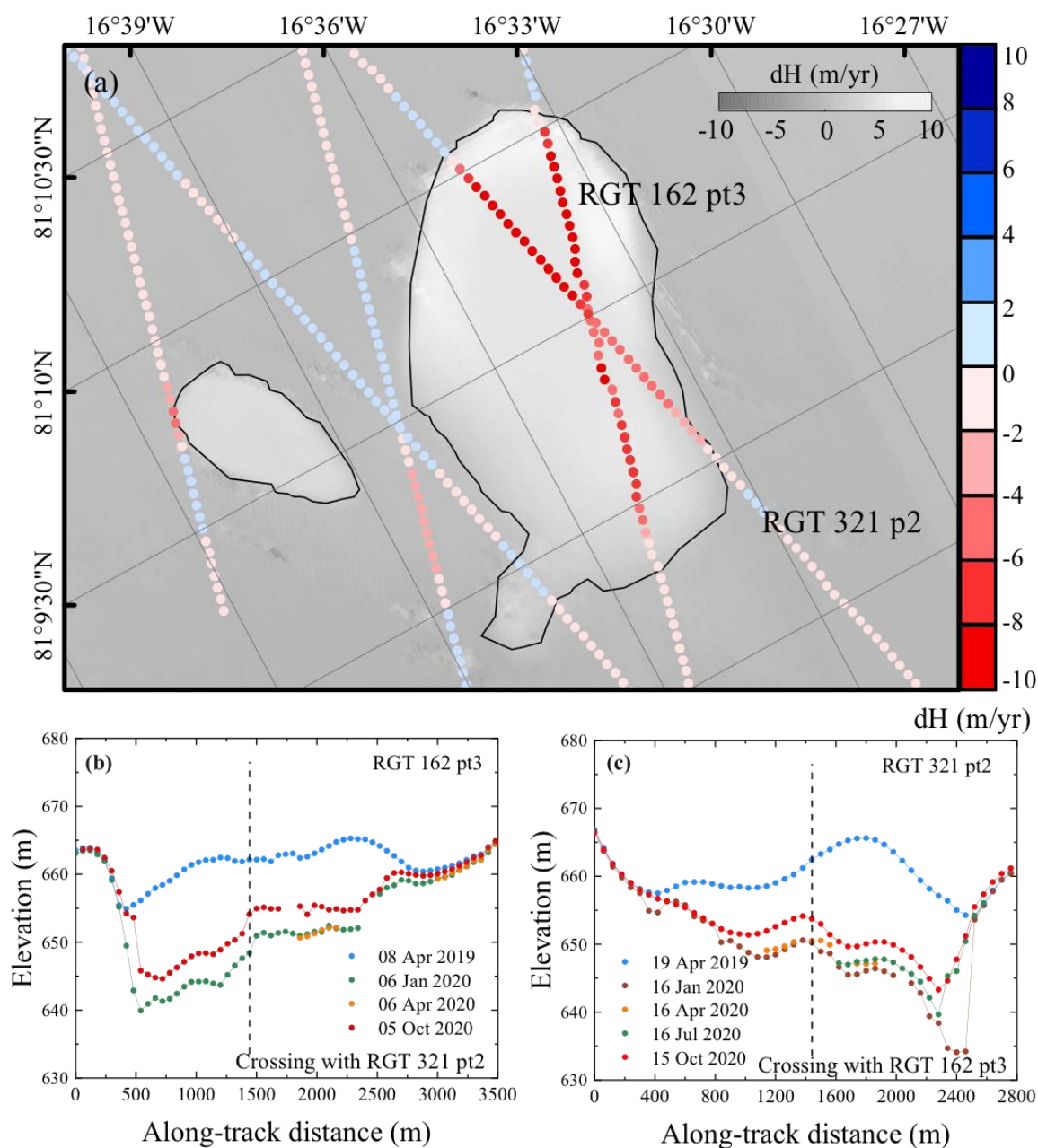


**Figure 1.** Active subglacial lake detection method, using Subglacial Lake ICE\_CAPS\_NE01 as an example. The elevation change rate was derived from ICESat-2 and overlaid on the elevation difference maps between the two ArcticDEMs (20160923-20160621). The black line shows the inferred lake boundary derived from the ArcticDEM (a). The red-blue colourbar stands for the ICESat-2, while grayscale colourbar stands for ArcticDEM. Elevation anomaly profiles across the subglacial lake along two ICESat-2 tracks (b) and (c). The colors of the points correspond to the ICESat-2 observation times, and the vertical dashed lines show the location of the cross point. Their spatial locations are also indicated in (a).

380

385



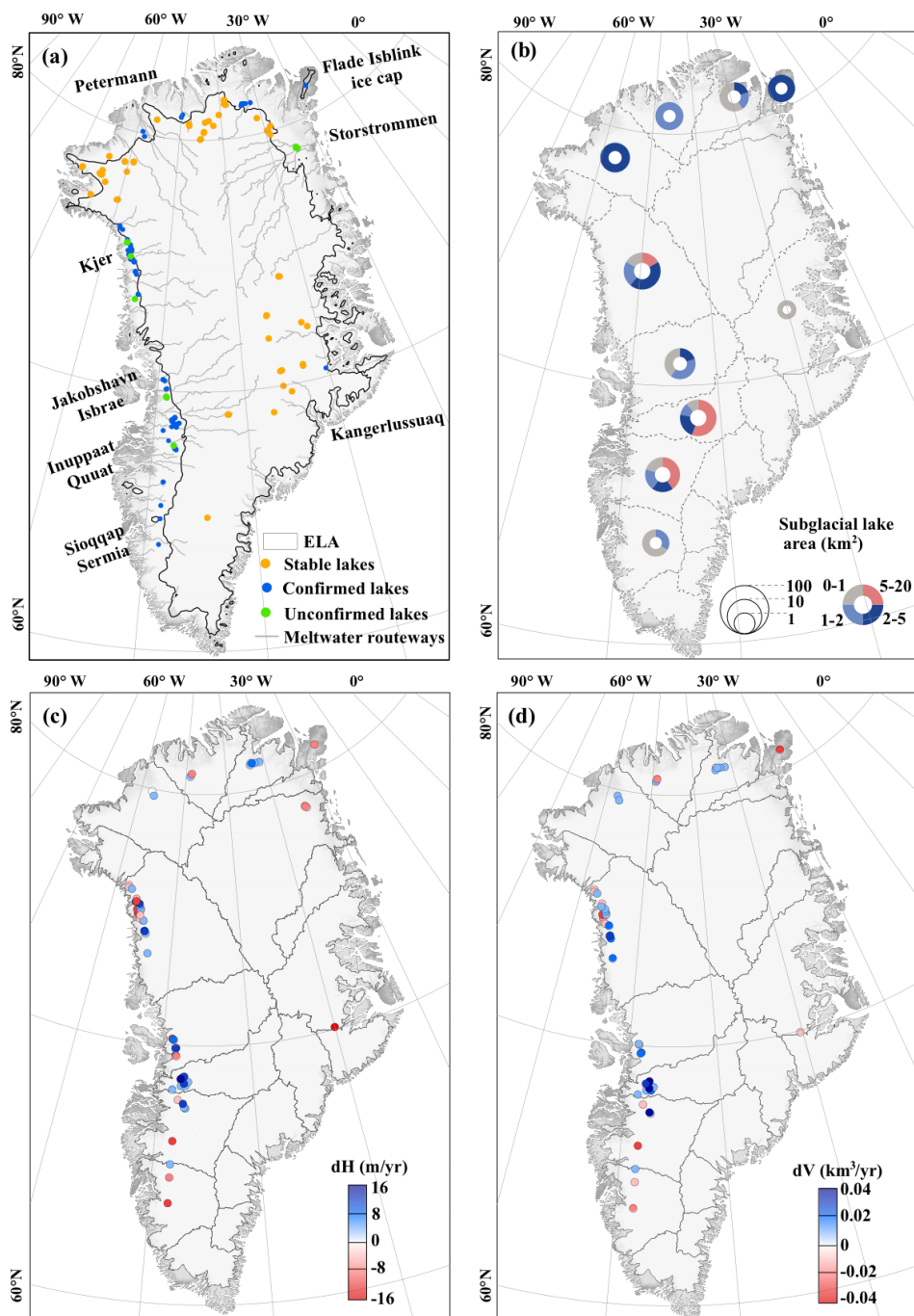


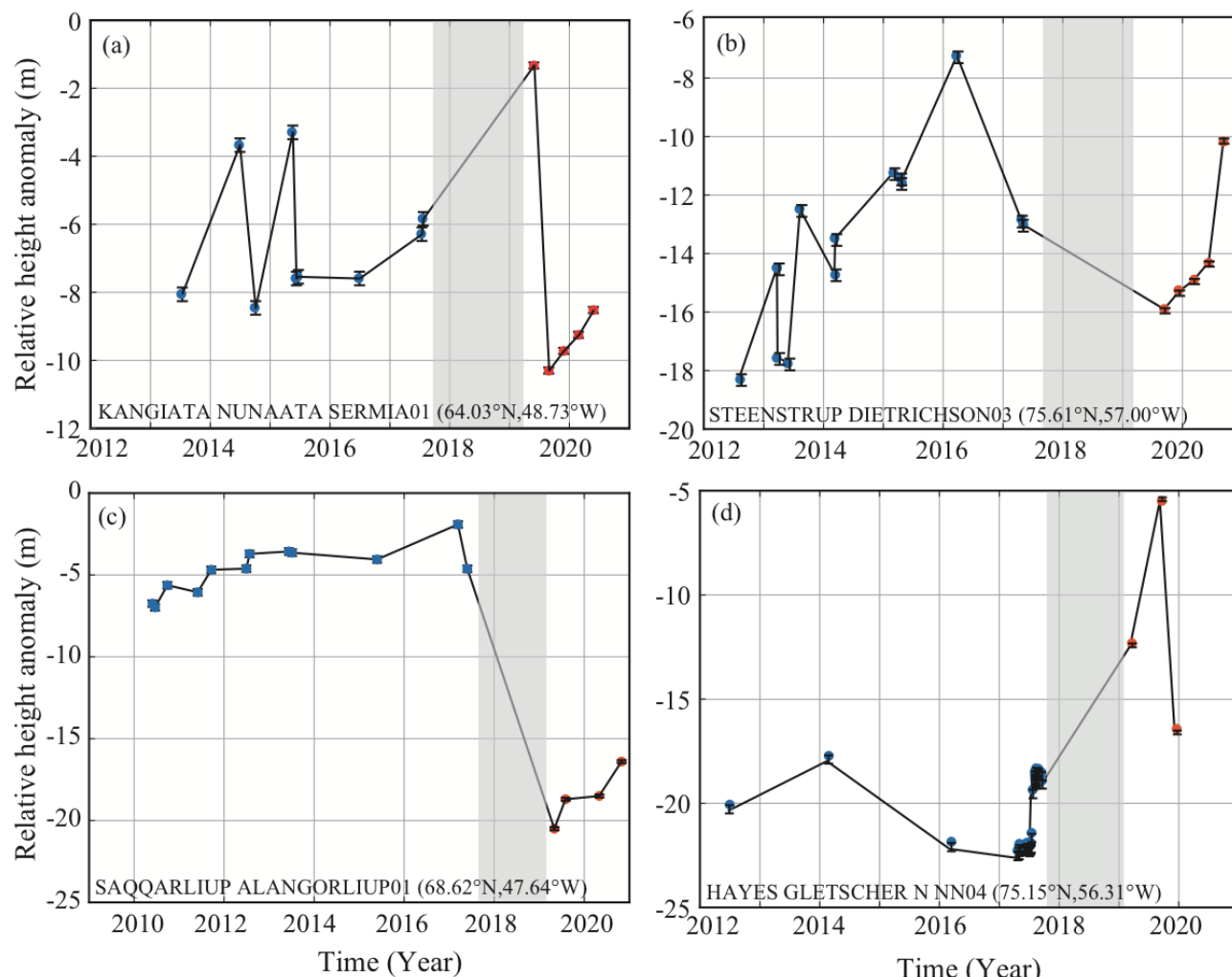
**Figure 2** Maps of the location (a), area (b), elevation change rate (c) and volume change rate (d) for the current active subglacial lakes under the Greenland Ice Sheet. The diameter in panel (b) is scaled by the total area of the active lake, with four sections representing the number of different lake size levels. Enlarged panels for the (c) and (d) can be found in Figure S5 and Figure S6 respectively. The meltwater pathways were derived from the hydraulic gradient (Livingstone et al., 2013), and the

390





Equilibrium Line Altitude (ELA) was derived from daily MARv3.12.1 data (Fettweis, et al., 2021) (a). Stable lakes in (a) are from Livingstone et al. (2022).



395 **Figure 3.** Time series of surface height change for four selected active lakes based on ArcticDEM (blue dots) and ICESat-2 tracks (orange dots). Each point represents the mean relative elevation difference between the lake and a 500 m buffer: (a) mode of slow filling and rapid draining, (b) mode of similar rates of filling and draining, and modes of long-term quiescence at a high stand (c) and low stand (d). Gray bar indicates the ArcticDEM/ICESat-2 data gap.